Journal of Mines, Metals and Fuels, *71(12C) : 307-314; 2023. DOI: 10.18311/jmmf/2023/47293*

Print ISSN : 0022-2755

Journal of Mines, Metals and Fuels

Contents available at: *www.informaticsjournals.com/index.php/jmmf*

Application of Direct Metal Laser Sintering for the Electrode Production and Study of Associated Process Parameters

S. Shashank[1*], Thomas Pinto[1], C. G. Ramachandra[2], M. Prashanth Pai[3], M. J. Raghavendra[1] and H. N. Reddappa[4]

[1]Department of Mechanical Engineering, Srinivas Institute of Technology, VTU, Belagavi – 590018, Karnataka, India; shashank.s844@gmail.com

[2]Deptartment of Mechanical Engineering, School of Engineering, Presidency University, Bengaluru – 560064, Karnataka, India

[3]Department of Mechanical Engineering, P.A. College of Engineering, VTU, Belagavi - 590018, Karnataka, India

[4]Department of Mechanical Engineering, Bangalore Institute of Technology, VTU, Belagavi - 590018, Karnataka, India

Abstract

The manufacturing sector is greatly influenced by the application of modern metal removal processes for the production of complex part geometries, the processes being non-conventional, versatile and more precise. Selective laser sintering is an additive manufacturing process which produces three-dimensional objects by fusing the powdered metal layer-by-layer in the presence of laser light. This work focuses on the manufacturing of electrodes by Direct Metal Laser Sintering and evaluating the influence of process parameters on the output responses under consideration. Laser power, scan speed, laser spot size, layer thickness, porosity and hatch spacing are the process parameters affecting the electrode production process. Sintering depth, energy density, relative density and ultimate tensile strength are the output responses. The experimental analysis examines the impact of the process parameters on sintering depth for the powdered Aluminium Alloy 6061. Optimised parameters are found to be 120W laser power, 285mm/s scanning speed, 15% porosity, 0.2mm laser spot size and 2.04mm layer thickness. Taguchi method is one of the techniques to obtain optimised electrode production by Direct Metal Laser Sintering.

Keywords: Laser Speed, Porosity, Scan Speed, Sintering Depth, Taguchi Method.

1.0 Introduction

In today's world mass production has gained a lot of importance. Businesses and industries strive for suitable technologies to produce high-quality components at low costs within the fixed time limits. Emerging in the 1980s, Additive Manufacturing (AM) enables the creation of complex three-dimensional solid parts through a layer-by-layer deposition method directly from digital data files. This process offers numerous advantages over conventional manufacturing methods, including design flexibility, reduced process times, minimized waste production and lower overall costs. AM represents a revolutionary shift in manufacturing, impacting engineering domains such as aerospace, mechanical, material and medical science and engineering. AM process control involving material deposition, fusing, melting, types of materials used and energy sources

**Author for correspondence*

involved in these processes. Initially, AM technologies[1] were characterised by stereolithography, fused deposition modelling, powder bed fusion[2], binder jetting and direct energy deposition. AM technologies utilise powders of metal/polymer to construct intricate 3-dimensional functional models or parts layer-by-layer, directly from Computer-Aided Design (CAD) data[3]. Energy sources such as laser beams or electron beams selectively sinter or melt the powdered materials. Direct Metal Laser Sintering (DMLS), a laser-based AM technique industrialized by EOS GmbH (Germany)[4]. It manufactures highly dense and precise metal parts. Rapid Prototyping (RP), is a key innovation (20th century) encompassing a series of fabrication techniques used to rapidly create, scale models of physical parts based on 3-dimensional CAD data. RP technologies facilitate the additive layer fabrication of parts[5], distinct from traditional subtractive manufacturing processes involving lathes, milling machines, etc. There are two primary RP approaches: the first creates prototypes directly, without requiring post-processing[6], while the second uses RP-generated parts to create moulds for prototype components. In AM and RP processes, surface roughness (R_a) is a critical parameter[7], but other important roughness parameters have often been overlooked in research analyses. The performance of the electrodes developed by RP technologies must be compared with the conventional ones under identical operative conditions[8]. Exploring hybrid Taguchi methods is essential for addressing multi-objective optimisation problems[9]. Preliminary studies have predominantly focused on achieving a lower Tool Wear Rate (TWR), higher Material Removal Rate (MRR) and lower R_a[10]. Key process parameters for DMLS and Electrical Discharge Machining (EDM) include scan speed, laser power, pulse on-time and off-time and sintering depth.

2.0 Methodology Adopted

The methodology includes the following sequential steps:

- Collection of necessary data from journals for preparation of electrode and material.
- Prepare the electrode using the DMLS process.
- Testing the scan speed and laser power of the DMLS electrodes.
- Performing EDM on samples in various machining conditions involving different combinations of process parameters like discharge current, pulse-on and pulse-off time, flushing pressure and workpiece material.
- Measuring Ra, TWR and MRR after each machining operation.

2.1 Selection of the Workpiece

Any material conducting electricity can be machined using EDM. The industrial and commercial sectors such as aeronautics, automobile and marine are finding increasingly important applications of AA 6061 aluminium alloy[11]. The abrasive nature of the reinforcing materials used in the composites can result in workpiece damage and cutting tool wear when the composites are machined using conventional machining processes[12]. EDM addresses these challenges by enabling precise machining of tough and wear-resistant materials, minimising tool wear and workpiece damage. The tool and the workpiece do not have a direct contact in EDM.

2.2 Choice of Tool Electrode

To apply EDM, one must use an electrically conductive tool electrode[13]. Frequently used tool electrode materials include copper, brass, graphite, tungsten carbides, copper-graphite alloys, etc. The electrodes manufactured by DMLS are also used as tool electrodes.

2.3 DMLS Tool Preparation

In DMLS, 3-dimensional geometries are created layer-by-layer. Direct Metal 20 (material) was used in the tool fabrication[14], with the help of the EOSINT 250 machine[15]. The machine includes a laser unit, a CPU, a powder distributor, a build chamber and a wiper blade. Magic RP software was used to design a 3-dimensional CAD model of the cylindrical specimen having a diameter and length of 20mm each[16]. EOS RP tools were used to slice the CAD model present in Stereolithography (STL) format. A constant layer thickness of 40µm was maintained. The process computer of the DMLS machine receives the sliced data whereas PSW software creates the laser path[17]. A base plate (steel) was attached to the build platform, which was heated to 80°C. Key process parameters include - laser power (228W), layer thickness (40µm), hatch width (5mm), hatch spacing (0.2mm) and laser scan rate (200 to 500mm/sec).

2.4 TWR and MRR Measurements

TWR and MRR are critical performance indicators in any machining operation[18]. Compared to conventional

machining, EDM typically exhibits lower TWR and MRR. High-accuracy weight scales are essential for measuring these performance indicators. For mass measurement, a digital scale (0.1mg accuracy) was utilised. After each experimental run, the material was removed and tool wear was found using the mass loss method. The mass of the tool and workpiece were measured thrice before and after machining to ensure accuracy and the average value was calculated. Additionally, the stopwatch was used to measure the machining time precisely.

2.5 Surface Roughness Test

To predict machining quality, it is essential to compute the R_a of the machined parts[14]. Each component's surface has a unique structure influenced by the technology used to manufacture it.

3.0 Results and Discussion

DMLS uses lasers to fabricate metal parts from powders, offering advantages over conventional manufacturing methods due to its cost-effectiveness and lower energy consumption. The process parameters are to be optimised to ensure high-quality parts[15]. Mathematical modelling can assist in identifying the optimal settings, ensuring the production of superior-quality parts. Understanding how these parameters influence the final product allows for continuous process improvement. In DMLS, a heat source of high intensity such as a laser, quickly melts and fuses powdered material[16]. A phase change occurs when the laser sufficiently heats the particles to melt them. As the molten material solidifies, it becomes denser and more compact, resulting in a robust structure. The high-quality parts with desired properties are obtained by carefully controlling and adjusting the process parameters. The DMLS process involves using a laser to melt selectively and bond powdered metal[17]. The laser scans over the powder bed according to the desired part geometry.

3.1 Testing on DMLS Based Electrode

Thermal analysis is crucial for enhancing the DMLS process as it reveals how various factors influence the final part[23]. These tests examine the transfer of heat through the powder bed during the application of laser. Thermal analysis provides valuable insights for process optimisation by the evaluation of parameters like laser power, scanning speed, spot size, layer thickness and porosity[18].

3.1.1 Laser Power

The laser controls how much energy goes into the powder. More laser power means more heat, which helps to melt and fuse the powder. However, too much power can cause problems like overheating or part distortion. Simulations help to find the best laser power to melt and fuse without causing damage.

3.1.2 Scan Speed

This decides how fast the laser moves over the powder. Quicker scans make the exposure time shorter. Performing heat tests can find the best scan speed to make sure the material melts and comes together properly, keeping the part quality good.

3.1.3 Laser Spot Size

The laser spot size influences the energy distribution of the powder and the quality of the melted area. Simulations can be performed to determine the optimal spot size for fusing the material for a specific application. By testing various spot sizes, the ideal parameters to obtain the preferred melting level and fusion can be identified.

3.1.4 Build Layer Thickness

The thickness of each layer affects the heating, cooling and stress in the part. Simulations help to analyse different layer thicknesses, leading to better part quality and accuracy.

3.1.5 Porosity Percentage

Pockets or air holes in the part indicate porosity which must be controlled to produce robust and high-quality components. Thermal simulations provide valuable insights into how different factors affect the formation of porosity.

3.1.6 The Hatch Spacing

The gap between the lines called hatch spacing, usually in millimetres or micrometres, changes based on the specific part being made. It affects the final part quality, accuracy, surface finish, build time and integrity of the part. Thermal simulations help to understand how the material behaves during DMLS. This is crucial to optimise the process parameters for making components with good mechanical properties and dimensional accuracy.

The process parameters listed in Table 1 significantly impact part quality, build time and mechanical properties. Table 2 includes them as the experimental input parameters in DMLS. These six parameters directly influence output responses such as sintering depth, energy density, relative density and ultimate tensile strength (Table 2). Optimisation of these parameters through experimental analysis is critical for achieving high-quality parts with desired performance characteristics in DMLS applications across diverse industries.

The optimisation of the DMLS process benefits significantly from advanced methodologies such as Taguchi and Response Surface Methodology (RSM). These techniques are pivotal in establishing and refining the relationships between key process parameters and critical output variables. Taguchi Method, renowned for its efficiency in experimental design, allows simultaneous variation of process parameters such as those listed in Table 1. By using orthogonal arrays and signal-to-noise ratios, the Taguchi Method identifies optimal parameter settings that minimize variability and maximise the desired sintering depth. The RSM describes the complex interactions between input parameters and output responses. RSM explores how variations in input parameters influence output responses. This integrated approach of Taguchi and RSM not only identifies influential factors but also quantifies their individual and combined effects on the manufacturing process.

3.2 Sintering Depth - Mean Effects Plot

Figure 1 presents the regression model aimed at maximising the sintering depth. The optimized process parameters as determined using MINITAB18 software include - laser power (120W), scan speed (285mm/s), porosity (15%) and build layer thickness (2.04mm).

Table 1. Experimental process parameters

		Levels		
Process Parameter	**Units**	**L1**	**L2**	**L3**
Laser Power	watts	80	100	120
Scan Speed	mm/s	95	190	285
Laser Spot	%	5	10	15
Porosity	mm	0.30	0.40	0.50
Build. Layer	mm	1.0	1.5	2.0
Hatch Spacing	mm	0.12	0.16	0.20

The response table (Table 3) for means shows how six factors (A-F) influence the response for sintering depth at three levels. The 'Delta' values indicate the range of means for each factor, highlighting the variability. Factor A has the highest impact on the response (Delta = 1.3867), followed by B, C, D, F and E. The 'Rank' column orders these factors by their impact, with 1 indicating the most significant. Table 3 helps to prioritise which factors to optimise using RSM.

3.3 Energy Density-Mean Effects Plot (MEP)

In the realm of DM20 electrode manufacturing, a mean effective plot as shown in Figure 2 visually demonstrates how varying individual process parameters influence the energy density. An experiment is designed to systematically investigate the range of relevant process parameters in the manufacturing of DM20 electrodes. For each combination of parameters, the energy density is measured to develop a regression model that accurately captures the relationship between these parameters and the response variable. The resulting energy density values are plotted on a mean effective plot. The approach allows for a clear interpretation of how specific process parameters influence the energy density and consequently, the quality and characteristics of the DM20 electrodes. By understanding these relationships, the process can be optimized to enhance efficiency and product quality.

The RSM for means as shown in Table 4 presents the effects of six factors (A-F) on the energy density at three different levels. The Delta row indicates the range of mean values for each factor, highlighting the variability in their impact. Factor E has the highest impact (Delta = 39.53), followed by A, B, F, C, and D. The 'Rank' column orders

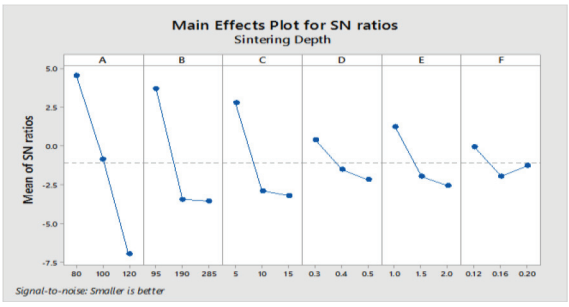


Figure 1. Mean effects plot for sintering depth (DMLS-based DM20 electrode)

Table 2. Experimental input and output response

Exp No.	Laser Power	Scan Speed	Laser Spot	Porosity	Build Layer	Hatch Spacing	Sintering Depth	Energy Density	Relative Density	UTS
	A-watts	B-mm/s	C-%	D-mm	E-mm	F-mm	X-mm	Y-J/mm^2	%	Mpa
1	80	95	5	0.3	1	0.12	0.02	42.56	93.26	180
2	80	95	5	0.3	1.5	0.16	0.3	60.63	93.46	190
3	80	95	5	0.3	2	0.2	1.02	80.99	93.56	200
4	80	190	10	0.4	1	0.12	1.65	44.6	95.22	190
5	80	190	10	0.4	1.5	0.16	1.75	62.45	95.35	200
6	80	190	10	0.4	2	0.2	0.35	82.78	95.46	210
7	80	285	15	0.5	1	0.12	0.65	46.78	97.45	200
8	80	285	15	0.5	1.5	0.16	1.2	64.57	97.56	210
9	80	285	15	0.5	2	0.2	1.85	84.98	97.88	220
10	100	95	10	0.5	1	0.16	1.95	50.77	94.55	210
11	100	95	10	0.5	1.5	0.2	0.4	70.45	94.55	230
12	100	95	10	0.5	2	0.12	0.88	90.78	94.66	260
13	100	190	15	0.3	1	0.16	1.35	52.45	95.61	230
14	100	190	15	0.3	1.5	0.2	1.56	72.33	95.78	260
15	100	190	15	0.3	2	0.12	1.77	92.25	95.89	280
16	100	285	5	0.4	1	0.16	0.56	54.2	96.77	250
17	100	285	5	0.4	1.5	0.2	1.02	74.63	96.87	270
18	100	285	5	0.4	2	0.12	1.65	94.76	96.98	290
19	120	95	15	0.4	1	0.2	1.75	60.12	97.77	270
20	120	95	15	0.4	1.5	0.12	2.82	80.23	97.87	300
21	120	95	15	0.4	2	0.16	1.03	100.12	97.98	320
22	120	190	5	0.5	1	0.2	1.75	62.23	98.12	300
23	120	190	5	0.5	1.5	0.12	2.23	82.36	98.14	340
24	120	190	5	0.5	2	0.16	2.45	102.45	98.17	380
25	120	285	10	0.3	1	0.2	2.89	64.45	99.22	340
26	120	285	10	0.3	1.5	0.12	3.1	84.6	99.31	375
27	120	285	10	0.3	2	0.16	3.25	104.79	99.34	395

Table 3. RSM for sintering depth

Response Table for Means						
Level	**A**	**B**	**C**	**D**	**E**	**F**
1	0.9767	1.13	1.2222	1.6956	1.3967	1.6411
2	1.2378	1.6511	1.8022	1.3978	1.5978	1.5378
3	2.3633	1.7967	1.5533	1.4844	1.5833	1.3989
Delta	1.3867	0.6667	0.58	0.2978	0.2011	0.2422
Rank	1	2	3	4	6	5

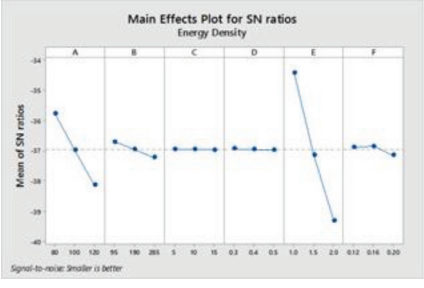


Figure 2. MEP for energy density.

these factors by their Delta values, with 1 being the most significant.

3.4 Relative Density - Mean Effects Plot

A mean effects plot for relative density in the manufacture of DM20 electrodes using DMLS (Figure 3) elucidates the effects of six factors on the response variable. Each factor may encompass multiple levels or categories, demonstrating how alterations in these levels influence the average relative density. Confidence intervals can be incorporated to denote the variability around the mean values.

The response table for means (Table 5) shows the effects of six factors (A-F) on the relative density at three levels. The Delta values indicate the range of mean responses for each factor, with Factor A showing the highest impact (Delta = 2.97), followed by B, C, D, E, and F. The Rank column orders these factors by their Delta values, with 1 being the most significant.

3.5 Ultimate Tensile Strength (UTS) - Mean Effects Plot

In the context of DMLS-based DM20 electrode manufacturing, Figure 4 represents a mean effects plot for Ultimate Tensile Strength (UTS). The plot depicts the factors which potentially influence UTS. Each factor may encompass multiple levels, illustrating how variations in these levels affect the average UTS. Confidence intervals may be included to denote variability around the mean values. The response table for means (Table 6) illustrates the impact of six factors (A-F) on UTS at three levels. Factor A shows the highest impact on UTS having a Delta value of 135.6, followed by factors B, E, D, C and F. The Rank column orders these factors by their Delta values, with 1 being the most significant.

3.6 Normal Probability Plot

Figure 5 helps to check the reliability of data by verifying whether the sintering depth values follow a normal distribution or not. A straight line means the data is normal.

The normal probability plot serves as a valuable visual aid to assess the distribution of sintering depths, highlighting deviations from normality within the set of data. It facilitates decision-making and helps in choosing suitable statistical approaches for subsequent analysis.

Figure 6 illustrates the energy distribution across various locations. A normal distribution of energy would manifest as a linear trend in the plot. A well-defined methodology aids in visualizing and validating the spread of energy. The dataset facilitates the selection of

Table 4. RSM for energy density

Response Table for Means						
Level	**A**	**B**	**C**	**D**	**E**	**F**
1	63.37	70.74	72.76	72.78	53.13	73.21
2	72.51	72.66	72.85	72.65	72.47	72.49
3	82.37	74.86	72.65	72.82	92.66	72.55
Delta	19	4.12	0.2	0.16	39.53	0.72
Rank	2	3	5	6	1	4

Table 5. RSM for relative density

Response Table for Means						
Level	**A**	**B**	**C**	**D**	**E**	**F**
1	95.47	95.3	96.15	96.16	96.44	96.53
2	95.74	96.42	96.41	96.7	96.54	96.53
3	98.44	97.93	97.09	96.79	96.66	96.58
Delta	2.97	2.64	0.94	0.63	0.22	0.05
Rank	1	2	3	4	5	6

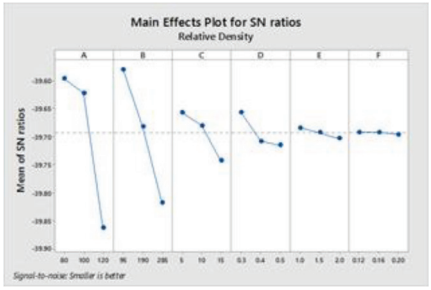


Figure 3. MEP for relative density.

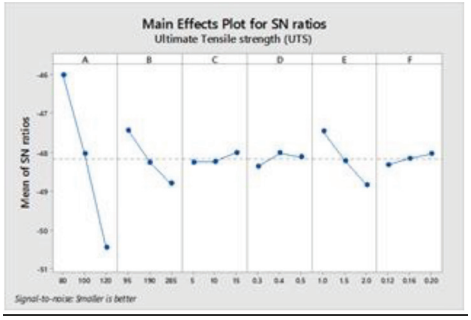


Figure 4. MEP for UTS table 6: RSM for UTS.

Table 5. RSM for UTS

Response Table for Means						
Level	**A**	**B**	**C**	**D**	**E**	**F**
1	200	240	266.7	272.2	241.1	268.3
2	253.3	265.6	267.8	255.6	263.9	265
3	335.6	283.3	254.4	261.1	283.9	255.6
Delta	135.6	43.3	13.3	16.7	42.8	12.8
Rank	1	2	5	4	3	6

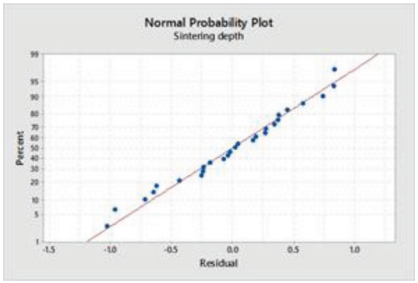


Figure 5. Normal probability plot - Sintering depth.

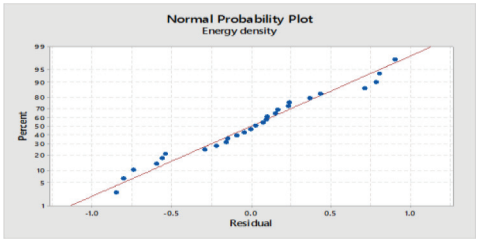


Figure 6. Normal probability plot - energy density.

appropriate statistical methods for further investigation and provides insights into the energy characteristics of DM20 parts.

The strength in DMLS, measured using the DM20 electrode, is assessed for normality as shown in Figure 7. In this graph, if the data points conform to a straight line, they ensure normal distribution. The observational approach ensures that the expected and observed data characteristics are aligned, which is crucial for selecting the appropriate statistical methods. Understanding the normality of the data enhances the quality assessment of measurements obtained from the DM20 electrode.

The analysis of UTS data obtained using the DM20 electrode serves as a tool to assess the normality of tensile strength distribution (Figure 8). A linear trend in the plot suggests adherence to a normal distribution. The graphical approach aids in assessing the consistency of UTS distribution with theoretical expectations, informing

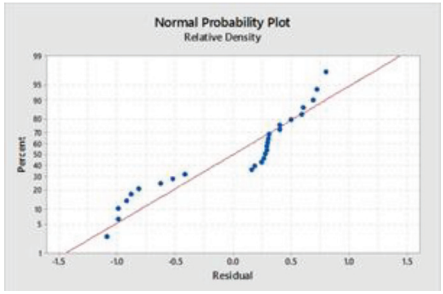


Figure 7. Normal probability plot - relative density.

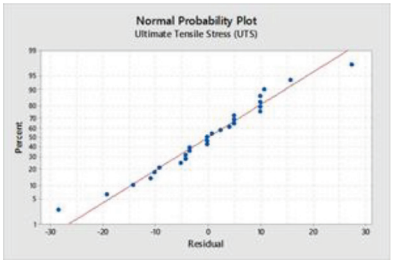


Fig. 8. Normal probability plot-UTS

the selection of appropriate statistical methods for further analysis. Adjustments to statistical methods may be necessary if deviations from normality are observed to ensure robust study results.

4.0 Conclusions

The study explores the influence of DMLS process parameters on sintering depth, energy density, relative density and UTS. The optimal DMLS settings for AA 6061 powder were identified as 120W laser power, 285mm/s scanning speed, 15% porosity, 0.2mm laser spot size and 2.04mm layer thickness. DMLS technology inherently provides good surface finish, stability and high precision. The approach aims to enhance the DMLS process by reducing the wastage of powder and increasing production efficiency. The Taguchi method can further improve the performance of DMLS electrode production.

5.0 References

1. Sivasankaran ST, Kumar S, Shanmugakani, Subbiah R. Performance analysis of conventional and DMLS copper electrode during EDM process in AA4032-TiC composite. Int J Adv Manuf Technol. 2022; 5:1423-8.
2. Equbal A, Equbal MI, Badruddin IA, Algahtani A. A critical insight into the use of FDM for the production of EDM

electrode. Alex Eng J. 2021; 61(5):4057-66. https://doi.org/10.1016/j.aej.2021.09.033
3. Strakaaivančorný L. Identification of geometric errors of circular profiles at WEDM caused by the wire tool electrode vibrations and their reduction with support of acoustic emission method. Eng Fail Anal. 2020; 134:106040. https://doi.org/10.1016/j.engfailanal.2022.106040
4. Machno M, Franczyk E, Bogucki R, Matras A, Zębala W. A comparative study on the structure and quality of SLM and cast AISI 316L samples subjected to WEDM processing. Int J Mach Tools Manuf. 2022: 15(3):701. https://doi.org/10.3390/ma15030701 PMid:35160647 PMCid: PMC8836433.
5. Amorim FL, Weingaertner WL. Die-sinking electrical discharge machining of a high-strength copper-based alloy for injection molds. J Braz Soc mech Sci. 2017; 26(2):137-44. https://doi.org/10.1590/S1678-58782004000200004
6. Amorim FL, Weingaertner WL. The behaviour of graphite and copper electrodes on the finish die-sinking electrical discharge machining (EDM) of AISI P20 tool steel. J Braz Soc Mech Sci. 2018; 29(4):1806-3691. https://doi.org/10.1590/S1678-58782007000400004
7. Raja P, Ramamoorthi G, Nallakumarasamy G. Experimental analysis and optimization of electrical discharge machining on titanium GR-2 with FEA. Int J Emerg Technol Eng Res. 2017; 5(7).
8. Cader M, Reid DT. Rapid prototyping and manufacturing: fundamentals of stereolithography. Society of Manufacturing Engineers. Dearborn, MI, USA. 2018. Jeff. Morgan Cristian Pisarciuc. A review of unconventional procedures for Manufacturing tool electrodes used in EDM. 2020; 15,3(43):205-8.
9. Brent EAP. Stucker, Bradley WL, Norasetthekul S, Eubank PT. The production of electrical discharge machining electrodes using SLS: Preliminary results. National Science Foundation Grant. 2021; 278-86.
10. Paolini AM. Rani I, Ketan. Optimization of various machining parameters of electrical discharge machining (EDM) Process on AISI D2 tool steel using hybrid optimization method. Int J Appl Innov Eng Manag. 2017; 3(9):2319-4847.
11. Ali MH, Levy GN, Schindel R, Kruth JP. Rapid manufacturing and rapid tooling with layer manufacturing (LM), state-of-the-art and future perspectives. CIRP Ann Manuf Technol. 2019; 52(2):589-609. https://doi.org/10.1016/S0007-8506(07)60206-6
12. Tarabeux OJ, Pateloup V, Michaud P, Chartier T. Resolution improvement of 3D stereo lithography through the direct laser trajectory programming: application to microfluidic deterministic lateral displacement device. J European Ceramic Society. 2018; 38(11):4089-98.
13. Samantaray, Gibson DW, Rosen BS. Additive manufacturing technologies. 3D printing, rapid prototyping and direct digital manufacturing, 2nd Edition, NewYork.
14. Song LX., Chen Z, Lei L, Shung K, Zhou Q, Chen Y. Piezoelectric component fabrication using projection-based stereolithography of barium titanate ceramic suspensions. J Rapid Prototyp. 2019; 23(1):44-53. https://doi.org/10.1108/RPJ-11-2015-0162
15. Dong, Felipe CM, Patrocinio D, Laza JM, Rubio LR, Vilela JLV. Evaluation of post-curing process on the thermal and mechanical properties of the Clear02™ resin used in stereolithography. J Polym Test. 2021; 72:115-21. https://doi.org/10.1016/j.polymertesting.2018.10.018
16. Hui A, Li M, Lu Z, *et al*. Research progress and direction of structural parameter optimization of pillar less sublevel caving in China. Metal Mine. 2020; (03): 1-11.
17. Zhou CB, Yao YK, Guo LW, *et al*. Numerical simulation of independent advance of ore breaking in the non-pillar sublevel caving method. China J University of Mining and Technology. 17(2). https://doi.org/10.1016/S1006-1266(07)60092-3. https://doi.org/10.1016/S1006-1266(07)60092-3